Original Article

The Correlation of Serum Adropin with Cardiovascular Risk Factors in the Experimental Rat Model of Chronic Kidney Disease and Its Implication in the Ameliorative Effect of Angiotensin-Converting Enzyme Inhibitors

Samaa Salah Abd-El-Fatah[1], MD; Maha A. Fathy[2], MD; Mohamed Ali Alabiad[3], MD; Raja Aljafil[4], MD; Mai Ahmed Gobran[3], MD; Enssaf A. Ahmad[1], MD; Ashwag S. Alsharidah[5], MD; Mohammed Alorini[6], MD; Sulaiman Mohammed Alnasser[7], MD; Sara A. Awadh[8], MD; Enas N. Morgan[2,9], MD

[1]Department of Anatomy and Embryology, College of Medicine, Zagazig University, Al-Sharquia, Egypt;
[2]Department of Medical Physiology, College of Medicine, Zagazig University, Al-Sharquia, Egypt;
[3]Department of Pathology, Faculty of Medicine, Zagazig University, Zagazig, Egypt;
[4]Department of Pathology, Faculty of Medicine, University of Benghazi, Benghazi, Libya;
[5]Department of Physiology, College of Medicine, Qassim University, Buraidah, Saudi Arabia;
[6]Department of Pathology, College of Medicine, Qassim University, Unaizah, Kingdom of Saudi Arabia;
[7]Department of Pharmacology and Toxicology, College of Pharmacy, Qassim University, Qassim, Saudi Arabia;
[8]Department of Biochemistry, College of Science and Art, King Abdelaziz University, Jeddah, Kingdom of Saudi Arabia;
[9]Department of Physical Therapy, College of Medical Rehabilitation, Qassim University, Buraidah, Saudi Arabia

Correspondence:
Mohamed Ali Alabiad, MD;
Department of Pathology, Faculty of Medicine, Zagazig University, Postal code: 44519, Zagazig, Egypt
Tel: +20 1150509554
Email: maabyad@medicine.zu.edu.eg
Received: 16 July 2023
Revised: 24 October 2023
Accepted: 19 November 2023

What's Known

• The risk of cardiovascular disease (CVD) in patients with chronic kidney disease (CKD) is estimated to be far greater than that in the general population.
• CKD is now considered an independent risk factor for CVD. Adropin has recently been demonstrated to regulate endothelial function and may play a role in the pathogenesis of CVD.

What's New

• Adropin levels are significantly correlated with most cardiovascular risk factors associated with CKD.
• It may be implicated in the ameliorative effect of angiotensin-converting enzyme inhibitors, possibly by affecting vascular endothelial growth factor receptor-2 and nitric oxide release.

Abstract

Background: The risk of cardiovascular disease (CVD) in patients with chronic kidney disease (CKD) is estimated to be far greater than that in the general population. Adropin regulates endothelial function and may play a role in the pathogenesis of CVD. Angiotensin-converting enzyme inhibitor (ACEI) treatment was reported to have a protective effect on both renal and cardiovascular function. This study investigated whether adropin is associated with renal and cardiovascular outcomes after using ACEI treatment in CKD rats.

Methods: In 2021, in Zagazig, Egypt, rats were assigned to: GI, control group (n=8); GII, CKD group (n=8), and GIII, CKD+captopril group (n=8), in which CKD rats received 100 mg/Kg/day captopril orally. Adropin levels, renal function, blood pressure, and various CVD risk factors were measured. Renal, cardiac, and aortic tissues were examined histologically and immunohistochemically to detect the expression of vascular endothelial growth factor receptor-2 (VEGFR-2). To analyze data, ANOVA and Pearson's correlation tests were used (SPSS version 18, P<0.05 is significant).

Results: Adropin was significantly lower in GII than in GI and GIII (P<0.001). Adropin in GII and GIII was negatively correlated with atherogenic index (P=0.019 and P=0.001, respectively), atherogenic co-efficient (P=0.012 and P=0.013, respectively), troponin I (P=0.021 and P=0.043, respectively), and nitric oxide (P=0.025 and P=0.038, respectively). VEGFR-2 expression decreased in GII and was elevated in GIII (P<0.001).

Conclusion: Adropin levels were significantly correlated with most CVD risk factors in CKD and captopril-treated CKD rats, indicating a role for adropin in the pathogenesis of CVD in CKD. It also refers to its implication in the ameliorative effect of ACEI treatment, possibly by affecting VEGFR-2 and nitric oxide release.

Introduction

The relationship between chronic kidney disease (CKD) and the risk of cardiovascular disease (CVD) is well-known; a high

percentage of patients with stage 4 to 5 CKD suffer from cardiovascular complications.[1] Moreover, CVD is the cause of death in 40%-50% of patients with stage 4 or 5 CKD, compared with only 26% of controls.[2] CVD risk is not restricted to the advanced stages of CKD, as patients in the earlier stages of CKD also have a high risk of subsequent coronary heart disease. Therefore, CKD is now considered an independent CVD risk factor, equivalent to coronary artery disorder in terms of the risk of all-cause mortality.[2]

The strong association between CKD and CVD is partly explained by traditional risk factors such as hypertension, metabolic disorders, and inflammation, which are all associated with progressive renal disease.[1] However, increasing evidence indicates a strong connection between proteinuria and CVD, both in patients with CKD and in the general population. Albuminuria is considered an index of the risk of cardiovascular or renal disorders.[1]

Adropin is a polypeptide hormone that regulates metabolism and energy homeostasis. It was identified in the liver, kidney, heart, small intestine, body fluids, and central nervous system.[3] Recent data have indicated that adropin deficiency is associated with insulin resistance, atherogenesis, and poor cell-to-cell communication. Serum adropin has recently been used as a marker of endothelial dysfunction.[3] Adropin levels were significantly correlated with the risk of coronary atherosclerosis in patients with diabetes and have been suggested as a potential predictor of coronary artery disorder.[3] Moreover, a relationship between adropin, kidney disease, and CVD was previously suggested. Lower levels of adropin were detected in hemodialysis patients, while another study considered low adropin levels to be an independent risk factor for CKD in diabetic patients with heart failure.[3]

The renin-angiotensin system (RAS) synthesizes angiotensin II (Ang II). Physiologically, Ang II plays a vital role in maintaining vascular tone, extracellular volume, and cardiac function. However, increased Ang II levels in CKD are associated with hypertension, renal injury, and risk of CVD.[4] Prolonged Ang II infusion over 1-2 weeks caused hypertension, increased reactive oxygen species output, increased preglomerular vascular resistance, and a decreased glomerular filtration rate as well as albuminuria, natriuresis, and glomerulosclerosis.[5]

Additionally, many studies have demonstrated a beneficial effect of angiotensin-converting enzyme inhibitor (ACEI) treatment in reducing renal tissue damage and CVD risk. ACEI treatment was found superior to other antihypertensive medications in preventing renal and cardiovascular

death in stage 3-5 CKD patients.[6] RAS blockade is supposed to exert benefits beyond lowering arterial blood pressure (ABP), which may include improvements in insulin resistance, inflammatory status, oxidative stress, and vascular function.[6]

The association between adropin and cardiovascular risk in CKD patients and its possible mechanisms needs further investigation. ACEI treatment is implicated in the management of both CVD and CKD, as previously mentioned. However, further investigation is needed to study the effect of ACEI treatment on adropin levels in CKD and whether adropin is associated with ACEI-induced effects on renal and cardiac function in CKD patients.

Therefore, this study aimed to examine the correlation of adropin levels with renal function and various risk factors for CVD, including hypertension, insulin resistance, proinflammatory markers, proteinuria, lipid profile, atherogenic index of plasma (AIP), atherogenic coefficient (AC), cardiac troponin I (cTnI), as well as oxidative radicals and D-dimer in an experimental model of CKD. In addition, the association of adropin with the outcomes of RAS blockade using an ACE inhibitor is investigated.

Materials and Methods

Animals

In total, 24 healthy adult male Wistar albino rats (182±20 g) were involved. The rats were provided by the Animal Center, College of Veterinary Medicine, Zagazig University, Egypt, and maintained throughout the study under hygienic conditions at the Animal House, College of Medicine, Zagazig University, Zagazig, Egypt. Rats were provided with free access to chow and water, kept at 21-23 °C on a 12-hour light/dark cycle and acclimated to animal house conditions for 2 weeks before experiments were begun.[7] This study was conducted in 2021 and followed the ARRIVE guidelines.[7] The Physiology Department Board and Institutional Animal Care and Use Committee of Zagazig University approved the study protocol (ref. ZU-IACUC/3/F/152/2021).

The rats were divided into three groups, GI-III (n=8 per group). In GI, the control group, rats were intraperitoneally injected with vehicle (0.2 mL of 0.3 mol/L NaHCO3) once a week for 5 weeks. In GII, the CKD group, rats were intraperitoneally injected with folic acid (MEPACO-MEDIFOOD, Egypt) at a dose of 240 mg/Kg dissolved in 0.2 mL of 0.3 mol/L NaHCO3 once a week for 5 weeks.[8] The mortality rate in this group was 20%; dead rats were replaced during the experiment. In GIII, the CKD+captopril group, rats received folic acid as for GII, plus 100 mg/Kg captopril

(E.P.I.C.O, 10th of Ramadan, Egypt) in 5 mL tap water administered by oral gavage daily for 5 weeks, beginning on day 1.[9] The mortality rate in this group was 12.5%; dead rats were replaced during the experiment.

At the end of the 5th week, metabolic cages were used to collect urine samples for 24 hours. Samples were measured for volume and centrifuged for 10 min at approximately 3000 rpm to purify the sample. The supernatant was stored at -20 °C.

ABP was measured using a PowerLab system (AD Instruments, Sydney, Australia) according to the manufacturer's instructions.[10]

Blood samples were withdrawn at the end of the 5-week experiment using the arterial blood pressure cannula after the ABP was measured. For each rat, approximately 3 mL of the withdrawn blood sample was collected in tubes containing 3.2% sodium citrate solution (0.1 mL: 0.9 mL blood) and centrifuged for 10 min at 1258 rpm. Plasma was used to measure the total cholesterol (TC), triglyceride (TG), high-density lipoprotein-cholesterol (HDL-C), and D-dimer levels. The remaining blood was used without anticoagulant to separate serum samples. The serum was isolated by allowing the blood samples to clot and then centrifuging at 3000 rpm for 20 min. Samples were stored at -20 °C.

Chemical Analysis

Serum adropin levels were analyzed using a rat adropin ELISA kit (Catalog no. 201-11-3361; Shanghai Sunred Biological Technology Co., Ltd., Shanghai, China).

Serum urea and creatinine and urine creatinine levels were measured using kits (Spinreact, Girona, Spain). Creatinine clearance was calculated using the following formula:
(urine creatinine×V)/serum creatinine[11]

Protein levels in the urine were assessed by measuring turbidimetry using a Microlab 300 (Vital Scientific B.V., Dieren, Netherlands).

Blood glucose levels were measured using a glucose enzymatic (GOD-PAP)-Liquizyme Rat Kit (Biotechnology, Egypt). Serum insulin levels were measured using a Rat ELISA kit (Catalog no. RAB0904; Merck, Darmstadt, Germany). The Homeostasis Model for Assessment of Insulin Resistance (HOMA-IR) was calculated using the following formula:
insulin (µIU/mL)×glucose (mg/dL)/405.[12]

C-reactive protein (CRP) levels were measured using a CRP kit (Monobind, Inc., Lake Forest, CA, USA). TC, TG, and HDL-C were measured using kits (BioSource Europe S.A., Nivelles, Belgium). AIP was calculated using the following formula:

log TG/HDL-C[13]

The atherogenic coefficient (AC) was calculated using the following formula:
(TC-HDL-C)/HDL-C[13]

Plasma cTnI and D-dimer levels were assessed using ELISA kits from Hangzhou Eastbiopharm Co., Ltd. (Hangzhou, China) and GenWay Biotech, Inc. (San Diego, CA, USA), respectively.

Serum nitric oxide (NOx) was determined using the Greiss reaction.[14] Serum levels of tumor necrosis factor α (TNFα; catalog no. RAB0480), interleukin-6 (IL-6), superoxide dismutase (SOD; catalog no. 19160), and malondialdehyde (MDA; Catalog no. MAK085) were measured using kits obtained from Merck, Germany.

Histopathological Examinations

Kidneys, hearts, and aortas were harvested from the rats. Kidney and heart specimens were fixed in 10% formal saline for 48 hours.[14-18] Simultaneously, abdominal aorta specimens were fixed in Bouin's solution for 48 hours. All the specimens were processed and embedded in paraffin blocks.[19-22] Sections 6-µm thick were stained with hematoxylin and eosin (H&E), Masson's trichrome, and immunohistochemical staining for vascular endothelial growth factor receptor-2 (VEGFR-2).

Pathological changes in the kidney, heart, and aortic sections were scored as previously described. For kidney sections, the grades were as follows: Grade 0: no pathological changes; Grade 1: cloudy swelling with pale cytoplasm in the tubules; Grade 2: tubulointerstitial pathology (tubular damage with loss of brush borders, detached epithelial cells, tubular casts, tubular sclerosis, and thickness of tubular basement membrane); Grade 3: glomerulonephritis with mononuclear inflammatory interstitial infiltration, glomerular mesangial cell hypercellularity, thickening of the glomerular capillary and blood vessel walls, and tubular necrosis; Grade 4: end-stage kidney disease with sclerosis of the glomeruli, tubules, thickness of the blood vessel wall, and extensive interstitial infiltration.

For heart sections, the grades were as follows: Grade 0: no pathological changes; Grade 1: cloudy swelling with pale cytoplasm in cardiac cells; Grade 2: mild myocarditis with mild inflammatory infiltration between myocardial cells (1-10 inflammatory cells per 10 high-power fields, ×400); Grade 3: moderate or severe myocarditis with 11-50 or >50 inflammatory cells per 10 high-power fields, respectively; Grade 4: myocardial scarring and necrosis of myocytes with minimal vascularity and inflammation.

For aortic sections, the grades were as

follows: Grade 0: no pathological changes; Grade 1: mild endothelial erosion and a few scattered red blood cells (RBCs); Grade 2: moderate endothelial erosion and adventitial hemorrhage; Grade 3: severe endothelial erosion and adventitial hemorrhage; Grade 4: narrow vasa vasorum, inflammation, and atheromatous plaque.

Masson's trichrome staining of collagen fibers was scored as follows: Grade 0: no stain (0%); Grade 1: mild staining (1-25%); Grade 2: moderate staining (26-50%); Grade 3: severe staining (>51%).

To detect the expression of VEGFR-2, 5-µm thick sections were cut. Antigen retrieval was achieved with 10 mM sodium citrate, and immunohistochemistry was performed as previously described.[23] Sections were graded as follows: Grade 0: negative (-ve); Grade 1: few positive cells (<25%), Grade 2: well-defined areas with positive cells (25-50%); and Grade 3: extensive areas with positive cells (>50%).

The entire sections were examined, photographed, and scored at magnification ×400 using a Leica DM500 light microscope (Leica Camera, Wetzlar, Germany) at the Anatomy Department, Faculty of Medicine, Zagazig University. The pathologist was blinded to the treatment.

Statistical Analysis

Data were normally distributed, so the parametric analysis was used, and values are expressed as mean±SD. Statistical analysis was performed using one-way analysis of variance (ANOVA), followed by *post hoc* analysis using the Least Significant Difference (LSD) test to compare means. Pearson's correlation coefficient was used to assess correlations between parameters. Pearson's Chi square test was used to confirm a statistically significant difference between the frequencies of grading between the groups. Significance was set at $P<0.05$. SPSS software version 18 (IBM Corp., Armonk, NY, USA) was used for the analysis.

Results

Chemical Analysis

Serum adropin levels were significantly decreased in GII compared with GI ($P<0.001$) and significantly increased in GIII compared with GII ($P=0.013$). However, the levels in GIII were significantly higher than those in GI ($P<0.001$).

Rats in GII had significantly increased serum creatinine, urea, and proteinuria, and significantly decreased creatinine clearance compared with those in GI. These parameters showed significant improvement in GIII compared with GII (table 1).

Table 1: Biochemical parameters and blood pressure measured in the control group, chronic kidney disease group, and chronic kidney disease+captopril group

Parameter	Control group-	Chronic kidney disease group	P value[a]	Chronic kidney disease +captopril group	P value[a]	P value[b]
Serum adropin (ng/mL)	30.98±3.78	19.69±2.64	0.001*	23.66±2.15	0.001*	0.013*
Serum creatinine (mg/dL)	0.85±0.12	3.01±0.57	0.001*	2.3±0.7	0.001*	0.014*
Blood urea (mg/dL)	39.2±4.7	152.8±29.5	0.001*	73.1±12.6	0.002*	0.001*
Creatinine clearance (mL/min)	0.69±0.06	0.34±0.07	0.001*	0.52±0.061	0.001*	0.001*
Proteinuria (mg/dL)	5.03±0.8	12.6±1.3	0.001*	9.8±1.9	0.001*	0.001*
Glucose (mg/dL)	93.6±9.3	159.8±18.7	0.001*	141.9±9.8	0.001*	0.014*
Insulin (µIU/mL)	12.1±1	15.2±1.7	0.001*	13.6±1.1	0.033*	0.019*
HOMA-IR	2.8±0.24	6.03±1.2	0.001*	4.8±0.57	0.001*	0.004*
TC (mmol/L)	2.16±0.13	3.86±0.12	0.001*	2.9±0.38	0.001*	0.001*
TG (mmol/L)	0.52±0.1	0.86±0.08	0.001*	0.64±0.08	0.013*	0.001*
HDL-C (mmol/L)	1.4±0.4	0.63±0.13	0.001*	1.03±0.32	0.023*	0.014*
AIP	-0.42±0.07	0.14±0.1	0.001*	-0.19±0.1	0.002*	0.001*
AC	0.66±0.4	5.36±1.5	0.001*	2.07±1.04	0.016*	0.001*
cTnI (ng/dL)	0.06±0.017	0.15±0.05	0.001*	0.11±0.03	0.01*	0.036*
D-dimer (µg/mL)	0.09±0.016	0.23±0.039	0.001*	0.11±0.04	0.285	0.001*
NOx (µmol/L)	23.8±3.5	14±1.8	0.001*	18.8±1.9	0.001*	0.001*
TNF-α (pg/mL)	18.2±4.1	55.4±8.9	0.001*	34.3±6.9	0.001*	0.001*
IL-6 (pg/mL)	107.4±9.7	234.3±29.8	0.001*	151.4±13.2	0.001*	0.001*
CRP (mg/mL)	0.51±0.024	1.8±0.14	0.001*	0.79±0.08	0.001*	0.001*
MDA (µmol/L)	9.8±1.6	18.2±1.7	0.001*	12.1±1.9	0.014*	0.001*
SOD (IU/mL)	211.5±16.6	121.3±8.3	0.001*	170.3±11.6	0.001*	0.001*
SBP (mmHg)	99.4±11.2	141.9±20.3	0.001*	113.5±12.2	0.076	0.001*
DBP (mmHg)	60.6±9	102.3±14.6	0.001*	63.8±8.3	0.577	0.001*

Values are expressed as mean±SD. ANOVA test was used, followed by LSD test. [a]Versus control group; [b]Versus chronic kidney disease group; *Significant, level of significance $P<0.05$

Serum adropin levels were inversely correlated with serum creatinine, blood urea, and proteinuria, and positively correlated with creatinine clearance in both GII and GIII (table 2).

There were significant increases in serum glucose, insulin, HOMA-IR, TC, and TG, and a significant decrease in HDL-C in GII compared with GI. These levels significantly improved after treatment with an ACEI in GIII (table 1). GII showed a significant negative correlation between serum adropin levels and levels of blood glucose, HOMA-IR, TC, and TG, and a positive correlation with insulin and HDL-C. The same results were recorded for GIII, except regarding insulin, where no significant correlation was observed (table 2).

AIP, AC, cTnI, and D-dimer levels were higher in GII than in GI. Their levels decreased significantly in GIII but remained significantly higher than those of the control group (table 1). There was a significant negative correlation between serum adropin levels and AIP, AC, cTnI, and D-dimer levels in GII. The same results were recorded for GIII, except for D-dimer levels, which showed no significant correlation (table 2).

Serum NOx levels were significantly reduced in the GII group compared with the control group. Levels were significantly elevated after treatment with captopril in GIII compared with GII; however, these did not return to baseline (table 1). There was a significant positive correlation between serum adropin and NOx levels in GII and GIII (table 2).

There was a significant increase in TNFα, IL-6, and CRP levels in GII compared with GI; these levels decreased significantly in GIII compared with GII (table 1). There was a significant negative correlation between serum adropin levels and serum TNFα and IL-6 levels in both GII and GIII, while CRP levels showed a significant negative correlation with adropin only in GII (table 2).

Concerning the oxidative stress markers, MDA was significantly increased, and SOD was significantly decreased, in GII compared with GI. In GIII, there was significantly reduced MDA and significantly elevated SOD compared with GII (table 1). Serum adropin levels were inversely correlated with MDA levels and positively correlated with SOD levels in GII and GIII (table 2).

There was a significant negative correlation between serum adropin levels and diastolic and systolic blood pressure in GII and GIII (table 2). Compared with GI, a significant increase in systolic and diastolic blood pressure was found in GII. There was a significant decrease in both levels in GIII compared with GII, and levels in GIII were not significantly different from levels in GI (table 1).

Table 2: Correlation between adropin levels and measured parameters in chronic kidney disease group and chronic kidney disease+captopril group

Parameter	Chronic kidney disease group		Chronic kidney disease+captopril group	
	r	P value	r	P value
Serum creatinine (mg/dL)	-0.884*	0.004	-0.753*	0.031
Blood urea (mg/dL)	-0.737*	0.037	-0.847*	0.008
Creatinine clearance (mL/min)	0.716*	0.046	0.856*	0.004
Proteinuria (mg/dL)	-0.713*	0.047	-0.713*	0.047
Glucose (mg/dL)	-0.713*	0.047	-0. 815*	0.014
Insulin (µIU/mL)	0.822*	0.012	0.415	0.306
HOMA-IR	-0.855*	0.007	-0.833*	0.01
TC (mmol/L)	-0.806*	0.016	-0.823*	0.012
TG (mmol/L)	-0.845*	0.008	-0.856*	0.007
HDL-C (mmol/L)	0.758*	0.02	0.846*	0.008
AIP	-0.792*	0.019	-0.929*	0.001
AC	-0.822*	0.012	-0.819*	0.013
cTnI (ng/dL)	-0.787*	0.021	-0.722*	0.043
D-dimer (µg/mL)	-0.816*	0.013	0.15	0.723
NOx (µmol/L)	0.772*	0.025	0.735*	0.038
TNF-α (pg/mL)	-0.816*	0.014	-0.837*	0.01
IL-6 (pg/mL)	-0.742*	0.035	-0.745*	0.034
CRP (mg/mL)	-0. 814*	0.014	0.342	0.408
MDA (µmol/L)	-0.831*	0.01	-0.783*	0.022
SOD (IU/mL)	0.779*	0.023	0.827*	0.011
SBP (mmHg)	-0.861*	0.006	-0.882*	0.004
DBP (mmHg)	-0.828*	0.011	-0.730*	0.04

r: Correlation with adropin; Pearson's correlation coefficient was used to assess correlations. *Significant correlation, level of significance: P<0.05.

Histopathological Analysis

H&E-stained sections of the renal cortex of GI animals represented typical characteristics (figure 1a). In contrast, examination of the left renal cortex of GII animals revealed glomerular collapse. Some glomeruli also showed glomerular sclerosis and a widening of the renal glomerular capsular space. There were multiple renal tubular injuries, such as flattening of the tubular epithelial lining, necrosis, sloughed cells in some tubular lumens, and loss of the brush border and vacuolization in the tubules. Some tubules were dilated and filled with a hyaline cast. Severe interstitial hemorrhage, inflammatory cellular infiltration, and congested blood vessels were observed (figure 1b). GIII kidneys showed normal glomeruli, and proximal and distal convoluted tubule cells were preserved to a certain degree. Some tubules showed sloughed epithelial cells, while others showed loss of the brush border and narrowing of the lumen lined with pale granular cytoplasm, indicating cloudy swelling of the kidney (figure 1c).

The cardiac muscle fibers from GI rats were normal (figure 1d), while those from GII animals showed inflammatory cellular infiltration of myocardial fibers with dilated vascular spaces containing RBCs, indicating myocarditis. (figure 1e). The cardiac sections from GIII animals showed typical features for most cardiac muscle fibers, with faint striations and central oval vesicular nuclei. However, pyknotic nuclei were still observed (figure 1f).
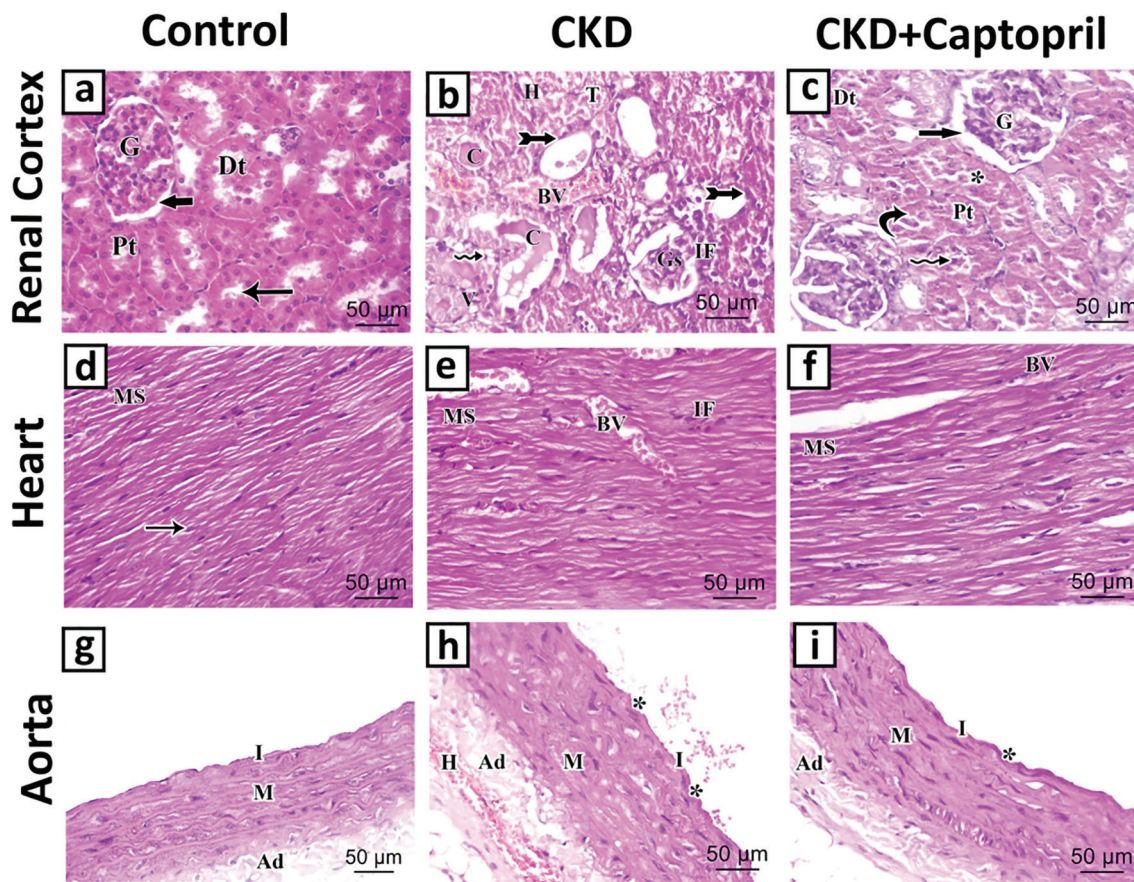

Figure 1: Representative photomicrographs of H&E-stained rat renal cortical tissues [a, b, c] for all studied groups showing a) GI: kidney has normal glomeruli (G) that contain a tuft of capillaries, Bowman's space (thick arrow), normal proximal tubule (Pt) with intact brush border (thin arrow), and distal tubule (Dt). b) GII: there is glomerular sclerosis (GS); some tubules are dilated and filled with hyaline casts (C). Tubular epithelial cells showed flattening (bifid arrows), sloughed cells into the tubular lumen (zigzag arrows), and apical vacuolation (V). The interstitium reveals severe interstitial hemorrhage (H) and inflammatory cell infiltration (IF). There is congestion of blood vessels (BV). c) GIII: glomeruli (G), Bowman's spaces (thick arrow), and proximal (Pt) and distal tubules (Dt) appeared typical. Some tubules showed detached epithelial cells (zigzag arrows), others showed loss of the brush border (curved arrow), and a narrow lumen lined by pale granular cytoplasm (*). Photomicrograph of H&E-stained cardiac tissues [d, e, f] of all studied groups. d) GI: there are longitudinally arranged cardiac muscle fibers with faint striations (MS) and central oval vesicular nuclei (arrows). e) GII: there is inflammatory cellular infiltration (IF)of myocardial fibers (MS) with dilated vascular spaces (BV) containing RBCs indicating myocarditis. f) GIII: Myocardial fibers (MS) appear nearly normal. Photomicrographs of H&E-stained aortic tissues [g, h, i] for all studied groups. g) GI: the walls of the blood vessel have normal intima (I), media (M), and adventitia (Ad). h) GII showing severe intimal (I) and endothelial injury and erosions (*). There are many RBCs in the lumen with hemorrhage (H) in the adventitia (Ad) and normal Media (M). i) GIII: the blood vessels showed minute erosion (*) of the intima (I) normal media (M) and adventitia (Ad). Scale bar=50 μm, ×400.

The aortic tissue from GI rats was normal (figure 1g), while those from GII animals showed severe endothelial injury and erosion. There were many RBCs in the lumen, with hemorrhage in the adventitia. In contrast, the medium appeared normal (figure 1h). The aortic tissue from GIII animals showed minute erosion of the intima with a few scattered RBCs in the lumen and typical media and adventitia (figure 1i).

Scoring of H&E-stained kidney sections revealed that grades 3 and 4 were highly represented in GII in comparison to both GI and GII, while grades 0 and 1 were significantly more frequent in GIII than in GII (table 3). Scoring of H&E-stained heart sections revealed that grades 3 and 4 were more common in GII than in GI and GIII, whereas grades 0 and 1 were significantly more frequent in GIII than in GII (table 4). Scoring of H&E-stained aorta sections revealed that grades 3 and 4 had a higher distribution in the aortic tissues of GII than in both GI and GIII, while grades 0 and 1 were significantly more

frequent in GIII than in GII (table 5).

Masson's trichrome staining showed fine collagen fibers within the renal cortex of animals of GI (figure 2a). In contrast, the kidneys of GII rats revealed a significant increase in collagen fiber distribution (figure 2b). GIII animals showed few collagen fibers within the renal cortex (figure 2c). Similar results were observed for hearts (figures 2d, e, f) and aortas (figures 2g, h, i) from GI, GII, and GIII animals, respectively.

VEGFR-2 Immunohistochemistry

Examination of VEGFR-2 immunohistochemical staining clarified the localization of positive cells in all experimental groups (as shown in figure 3). The staining was localized in the cytoplasm of the affected tissues. In the control groups, the renal cortex, heart, and aorta sections revealed moderate immunoreactions against VEGFR-2. In contrast, GII showed few VEGFR-2 immunopositive reactions. However, GIII sections were strongly VEGFR-2 immunopositive.

Table 3: Histopathological scoring of kidney section for H&E-stained slides

Grade	GI (n=8)	GII (n=8)	GIII (n=8)	Chi square test	P value
	N (%)	N (%)	N (%)		
0: Normal	8 (100%)	0 (0%)	1 (12.50%)	9	0.0027*
1: Cloudy swelling	0 (0%)	0 0%	7 (87.50%)		
2: Tubular-interstitial disease	0 (0%)	0 0%	0 (0%)		
3: Glomerulonephritis	0 (0%)	1 (12.50%)	0 (0%)		
4: End-stage kidney failure	0 (0%)	7 (87.50%)	0 (0%)		

*Significant (P<0.05); GI: The control group; GII: The chronic kidney disease group; GIII: The chronic kidney disease+captopril group

Table 4: histopathological scoring of heart sections for H&E-stained slides

Grade	GI (n=8)	GII (n=8)	GIII (n=8)	Chi square test	P value
	N (%)	N (%)	N (%)		
0: Normal	8 (100%)	-	6 (75%)	4	0.0455*
1: Cloudy swelling	-	-	2 (25%)		
2: Mild myocarditis	-	-	-		
3: Moderate and severe myocarditis	-	2 (25%)	-		
4: Myocardial scar	-	6 (75%)	-		

*Significant (P<0.05); GI: The control group; GII: The chronic kidney disease group; GIII: The chronic kidney disease+captopril group

Table 5: Histopathological scoring of aorta sections for H&E-stained slides

Grade	GI (n=8)	GII (n=8)	GIII (n=8)	Chi square test	P value
	N (%)	N (%)	N (%)		
0: Normal	8 (100%)	0 (0%)	1 (12.5%)	4	0.0455*
1: Mild endothelial erosion, few scattered RBCs	0 (0%)	0 (0%)	6 (75%)		
2: Moderate endothelial erosion, adventitial hemorrhage	0 (0%)	1 (12.5%)	1 (12.5%)		
3: Severe endothelial erosion, adventitial hemorrhage	0 (0%)	1 (12.5%)	0 (0%)		
4: Narrow vasa vasorum, inflammation, atheromatous plaque	0 (0%)	6 (75%)	0 (0%)		

*Significant (P<0.05); GI: the control group; GII: the chronic kidney disease group; GIII: the chronic kidney disease+captopril group
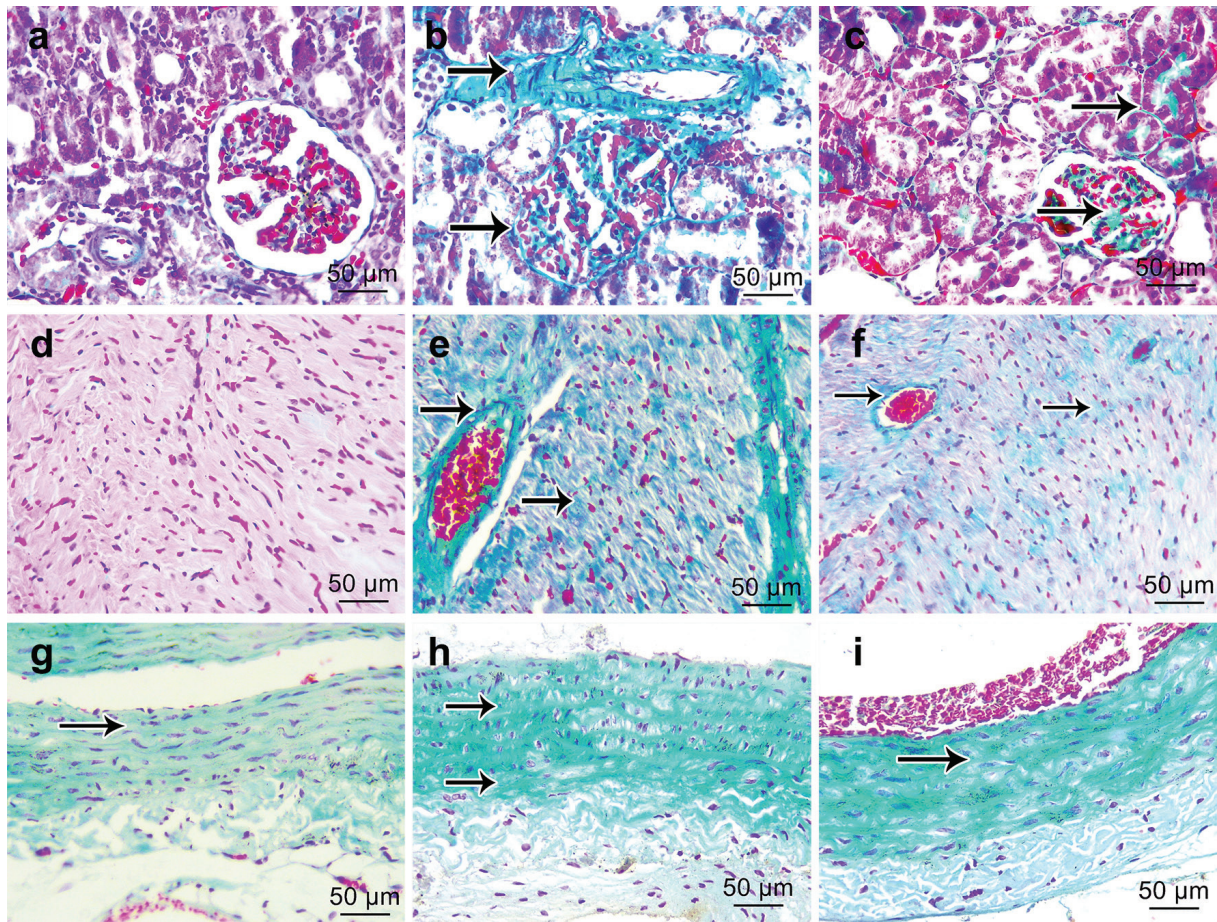
Figure 2: Different experimental groups showed Masson's trichrome-stained renal cortex, cardiac, and aortic sections. Control groups (a, d, and g, respectively) show fine collagen fibers (arrows) within the renal cortex, cardiac, and aorta tissue. On the contrary, CKD groups (b, e, and h, respectively) revealed a significant increase in collagen fibers (arrows) within tissues. However, CKD+captopril groups (c, f, and I, respectively) showed few collagen fibers (arrows) within the renal cortex, heart, and aorta tissue. Masson's trichrome, Scale bar=50 μm, ×400.

Table 6: Grading of Masson's trichrome and VEGFR-2 staining of kidney, heart, and aortic sections

	GI-Masson's		GI-VEGFR-2		GII Masson's		GII VEGFR-2		GIII Masson's		GIII VEGFR-2		Chi square test	P value
	n	%	n	%	N	%	n	%	N	%	n	%		
G0-K	8	100	0	0	0	0	3	37.5	3	37.5	0	0	11.733	0.01*
G1-K	0	0	6	75	1	12.5	5	62.5	5	62.5	0	0		
G2-K	0	0	2	25	1	12.5	0	0	0	0	1	12.5		
G3-K	0	0	0	0	6	75	0	0	0	0	7	87.5		
G0-H	8	100	1	12.5	0	0	6	75	6	75	0	0	10.707	0.03*
G1-H	0	0	6	75	0	0	1	12.5	2	25	0	0		
G2-H	0	0	1	12.5	3	37.5	1	12.5	0	0	2	25		
G3-H	0	0	0	0	5	62.5	0	0	0	0	6	75		
G0-A	8	100	0	0	0	0	2	25	2	25	0	0	24.736	0.001*
G1-A	0	0	5	62.5	1	12.5	6	75	6	75	1	12.5		
G2-A	0	0	3	37.5	2	25	0	0	0	0	1	12.5		
G3-A	0	0	0	0	5	62.5	0	0	0	0	6	75		

*Significant (P<0.05); GI: the control group; GII: the chronic kidney disease group; GIII: the chronic kidney disease+captopril group; A: Aorta; H: Heart; K: Kidney; VEGFR-2: vascular endothelial growth factor receptor-2

Masson's trichrome staining scores of kidney and cardiac and aortic sections revealed a significantly higher incidence of grades 2 and 3 in GII than in both GI and GIII. GIII had a higher frequency of Grades 0 and 1 than GII (table 6).

Scoring of VEGFR-2 expression in kidney, cardiac, and aortic sections revealed significantly higher grades 0 and 1 in GII than in GI, which showed significantly more grades 1 and 2, while GIII had a significantly higher proportion of grades 2 and 3 than G1 and GII (table 6).
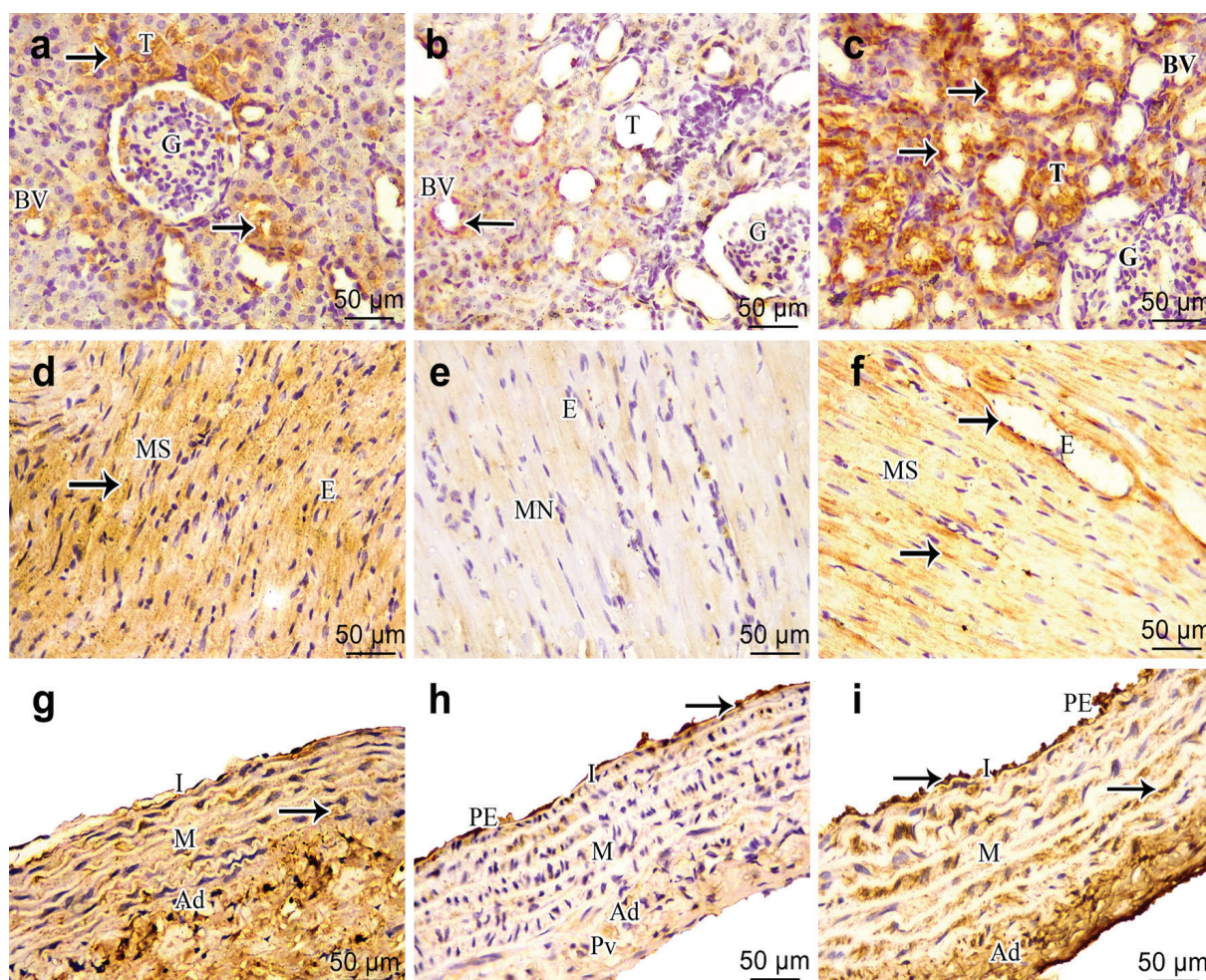
Figure 3: Representative photomicrographs of immunohistochemical analysis with VEGFR-2 antibodies of rat renal cortical tissues [a, b, c] in all studied groups. (a) GI showing moderate expression of VEGFR-2 (brown cytoplasmic stain (arrows) in Glomerular capillaries wall (G) with, Tubular basement membrane (T). Positive endothelial cells in the lining of the blood vessels (BV). (b) GII showing mild positive expression of VEGFR-2 in Glomerular capillaries wall (G), Tubular basement membrane (T), and negative endothelial cells in the lining of the blood vessels (BV). (c) GIII revealed marked expression of VEGFR-2 in the Glomerular capillaries wall (G), Tubular basement membrane (T), and positive endothelial cells in the lining of the blood vessels (BV). Representative photomicrographs of immunohistochemical analysis with VEGFR-2 antibodies of rat heart tissues [d, e, f] of 5 weeks studied groups. (d) GI showing moderate positive expression of VEGFR-2 in the vascular spaces endothelial lining (E) within the muscle (MS) longitudinal section. (e) GII showing mild expression of VEGF within the endothelial lining (E) of the vascular spaces within the longitudinal section of muscle cells revealing areas of muscle necrosis (MN). (f) GIII showing the marked expression of VEGR-2 in the endothelial lining of the vascular spaces (E), and muscle cells (MS) in the longitudinal section. Representative photomicrographs of immunohistochemical analysis with VEGFR-2 antibodies of rat aortic tissues. (g) GI showing moderate expression of VEGFR-2 in the endothelium of intima (I), media (M), and adventitia (Ad). (h) GII showing mild expression of VEGFR-2 with positive brown staining (Arrow) of the endothelium (PE) and also in the intima (I), media (M), and adventitia (Ad). Adventitia reveals also positive vasa vasorum lining (PV). (i) GIII showing marked expression of VEGFR-2 with (brown cytoplasmic stain (arrows) in the endothelium (PE) of intima (I), normal media (M), and adventitia (Ad). VEGFR-2, Scale bar=50 µm, ×400.

Table 7: Diagnostic performance of Masson's trichrome and VEGFR-2 staining of kidney, heart, and aortic sections

	Masson's trichrome Kidney	Masson's trichrome Heart	Masson's trichrome Aorta	VEGFR-2 Kidney	VEGFR-2 Heart	VEGFR-2 Aorta
Sensitivity	100%	100%	100%	100%	100%	100%
Specificity	81.82%	94.12%	81.82%	100%	89.19%	78.12%
Positive predictive value	77.78%	87.50%	77.78%	100%	79%	50%
Negative predictive value	100%	100%	100%	100%	100%	100%
Positive likelihood ratio	5.50	17.00	5.50	100%	9.25	4.75
Negative likelihood ratio	0.0	0.0	0.0	100 %	0.0	0.0
Accuracy	92%	94.12%	89%	100%	92.31%	82.50%

VEGFR-2: Vascular endothelial growth factor receptor-2

Both Masson's trichrome and VEGFR-2 staining of kidney, cardiac, and aortic sections showed high sensitivity (100%) in all tissues (table 7). VEGFR-2 staining showed the highest specificity and accuracy for kidney lesions (100%).

Discussion

This study revealed an association between serum adropin and cardiovascular risk factors in CKD rats, which potentiates the claims of its possible involvement in the pathogenesis of both CVD and CKD. Treatment of CKD rats with ACEI was accompanied by a significant increase in adropin level that was correlated with most renal and cardiovascular parameters, a finding that refers to a role for adropin in ACEI-induced effects.

Adropin levels decreased in GII compared with the control group, and these levels were negatively correlated with creatinine, urea, proteinuria, glucose, HOMA-IR, TC, TG, TNFα, IL-6, AI, AC, cTnI, D-dimer, and MDA, in addition to a direct correlation between adropin levels and creatinine clearance, and serum levels of insulin, HDL-C and SOD. Similarly, adropin has previously been shown to cause a significant decrease in TNFα and IL-6 mRNA expression in the pancreatic tissue of diabetic rats.[24] Moreover, adropin levels were inversely correlated with TNFα levels in women with polycystic ovarian syndrome,[25] indicating an anti-inflammatory effect of adropin. A similar study revealed a possible complex association between adropin and the cardiovascular status of patients with CKD, as it demonstrated a significant direct correlation between adropin and cTnI and N-terminal pro-B-type natriuretic peptide.[26]

Administration of captopril in GIII alongside a high dose of folic acid reduced the adverse effects caused by the latter. Captopril improved renal function parameters; there was a significant decrease in serum urea and creatinine levels, as well as reduced proteinuria levels and increased creatinine clearance. Histopathological examination of the renal tissues showed normal glomeruli and proximal and distal convoluted tubules; H&E staining revealed a significantly higher proportion of grades 0 and 1 than in GII. Similar to our results, ACEI treatment was previously reported to improve renal tissue damage, decrease CVD risk, and prevent renal and cardiovascular death in stage 3-5 CKD patients, and its effect was even found superior to other antihypertensive medications.[11]

RAS blockade has a beneficial effect beyond lowering ABP, including improvements in insulin resistance, inflammation, oxidative stress, and vascular function.[6] The metabolic parameters and the values of AIP, AC, cTnI, D-dimer, CRP, proinflammatory cytokines, oxidative stress radicals, and arterial blood pressure were significantly improved after captopril treatment in the present study. In addition to the improvement in the histopathological appraisal of cardiac and aortic tissues compared with that of GII, Masson's trichrome staining showed fewer collagen fibers within the renal cortex, cardiac, and aortic tissues than GII. Captopril may improve hemodynamic status by upregulating NOx, as serum NOx levels were significantly elevated in GIII compared with GII. This NOx elevation may be due to the direct effect of captopril or through the increase in adropin levels recorded after captopril treatment. Vasodilation and control of myocardial oxygen consumption by NOx may significantly contribute to the therapeutic effect of ACEI in cardiac disorders, as ACEI can decrease kinin degradation and increase NOx formation.[27]

Adropin has also been shown to have anti-inflammatory and regulatory effects on the endothelium and was recently used to control endothelial cell function by upregulating endothelial NOx synthase (eNOS) expression through the VEGFR2-PI3K/Akt and VEGFR2-ERK1/2 pathways. Lower adropin levels have been shown to lead to endothelial dysfunction, which is a significant early event in atherogenesis and the onset of CVD.[3] Similarly, low serum adropin levels have been presented as an independent predictor of coronary atherosclerosis. Through suppression of inflammation, cellular migration, and adhesion, adropin can inhibit atherosclerosis either by direct anti-inflammatory effect or by boosting endothelial NOx production,[28] which remains to be determined. In the present study, the levels of adropin in the CKD group were directly correlated with NOx levels, which have a substantial role in generating and mediating complicated hemodynamic disorders associated with the progression of CKD.[29] In the present study, GIII showed higher VEGFR-2 expression in renal, cardiac, and aortic tissues than GII. Activated VEGFR-2 can evoke endothelial cells to form NOx, primarily via the PKC-PI3K/Akt pathway. VEGFR-2 mediated signals can enhance eNOS binding to its molecular chaperone heat shock protein 90 and boost endothelial NOx release. VEGFR-2 activation can also control blood pressure by increasing the permeability of blood vessels and relaxing vessel walls.[30] In the present study, the CKD group showed higher systolic and diastolic blood pressures than the control group with a

negative correlation between adropin levels and systolic and diastolic ABP in both GII and GIII. Similarly, a previous study demonstrated reduced adropin levels in hypertensive patients with blood pressure values exceeding 180/110 mmHg compared with normotensive controls.[31]

There is a strong association between CVD and CKD owing to their mutual traditional risk factors, such as disturbances in carbohydrate and lipid metabolism, inflammation, or increased oxidative radicals.[3] Our results revealed significantly disturbed metabolic parameters in the CKD group, as there were significantly elevated glucose, insulin, HOMA-IR, TC, and TG levels with a considerable reduction in HDL-C compared with the control group. Many studies have suggested that patients with CKD have carbohydrate metabolism disturbances and hypothesized that insulin resistance might be responsible for high cardiovascular morbidity and mortality in patients with CKD.[32] Impaired glucose oxidation, impaired suppression of endogenous glucose production, and abnormal insulin secretion influence glucose intolerance in CKD, and these carbohydrate metabolic disturbances may be due to the accumulation of nitrogenous uremic toxins.[33]

The malnutrition-inflammation complex syndrome developed in CKD patients may lead to a low body mass index, hypocholesterolemia, hypohomocysteinemia, and other manifestations of lipid metabolic dysfunction.[34] The contribution of dyslipidemia to the risk of cardiovascular complications in patients with CKD was previously reported, and CKD-associated dyslipidemia was found highly atherogenic.[35] Matching with our results, CKD patients are commonly found with elevated serum TG and low HDL-C levels, which are negatively correlated with the risk of atherosclerosis.[35]

Regarding inflammatory mediators and oxidative stress radicals, the present study showed a significant increase in TNFα, IL-6, CRP, and MDA levels, and a significant decline in the levels of SOD in GII compared with GI. These results are in accordance with previous studies that indicated inflammation is a crucial process in patients with CKD; therefore, CKD is considered a systemic inflammatory condition.[36] Pro-inflammatory processes in CKD patients may be due to various factors, including infection, insulin resistance, metabolic acidosis, oxidative stress, and reduced cytokine clearance.[36]

The AIP and AC are practical formulas for predicting the risk of CVD. AIP is based on two influential lipids: TG and HDL-C. In contrast, AC represents the ratio of non-HDL-C to HDL-C.[19] Both indices quantify blood lipid levels and are considered optimal indicators of dyslipidemia and the associated cardiovascular risk.[37] The present study results revealed an increase in the AIP and AC, which were negatively correlated with adropin in the CKD group compared with the control group, indicating a high risk of CVD in this group. This finding is in accordance with earlier studies that reported a significant increase in AIP in chronic renal patients.[29]

Moreover, cTnI and D-dimer levels were higher in the CKD group than in the control group. Many experimental studies have demonstrated that cTnI is released due to irreversible cell death.[38] However, other studies have shown that myocardial ischemia alone could result in cTnI release without evidence of necrosis, and reversible cell damage can increase its release by releasing membranous blebs; neither mechanism has been confirmed to date.[37, 38] Recent evidence identified D-dimer as a useful marker to predict cardiovascular complications and mortality.[39]

As explained above, biochemical analysis showed a high probability of CVD in GII due to multiple interactive risk factors. Masson's trichrome staining scores of kidney, cardiac, and aortic sections revealed a significantly higher ratio of grades 2 and 3 in GII than in the control group. Histological analysis of the cardiac muscle indicated a higher ratio of grades 3 and 4, including myocarditis and cardiac scars, respectively, in GII. In addition, GII aortic tissues showed pathological changes extending from moderate and severe endothelial erosion with adventitial hemorrhage to narrowing of the vasa vasorum and atheromatous plaque.

A possible mechanism may be the reduced endothelial synthesis of NOx in CKD. Appropriately functioning eNOS is essential for controlling arterial pressure, glucose, and lipid homeostasis.[39] Inadequate NOx synthesis in the kidneys is crucial for generating and mediating the complicated hemodynamic disturbances associated with CKD progression.[28] The present study indicated a significant decrease in serum NOx in GII. These results align with the reduced daily excretion of urinary nitrite/nitrate previously detected in patients with moderate to severe CKD compared with those with mild CKD and healthy controls.[40] Lack of NOx may result from decreased arginine levels since the kidney is an important site for endogenous arginine synthesis.[28]

Our study focused on the correlation between adropin and different measured renal and cardiovascular parameters, but it lacks the investigation of different cellular and molecular pathways that explain our results. Studying the effect of *in vivo* adropin administration is also

needed to confirm the outcomes of the study, which was another limitation of our work.

Conclusion

In this study, adropin levels were significantly correlated with most of the risk factors analyzed. ACEI treatment in CKD rats was associated with a significant increase in adropin level that was correlated with most renal and cardiovascular parameters, indicating a role for adropin in the ameliorative effect of ACEI treatment probably by up-regulating VEGFR-2 in cardiac, renal, and aortic tissues and boosting endothelial NOx release. However, the exact mechanism of its function and regulation remains to be determined. Further clinical and experimental studies that go beyond correlative analyses will be required to define the exact role of adropin in the pathophysiology of CVD risk.

Acknowledgment

Authors' Contribution

SS. A: Study concept, study design, data gathering, data analysis, drafting; MA.A: Study concept, study design, data gathering, data analysis, drafting and reviewing the manuscript; MA.F; R.A; MA.G; EA.A; AS.A; M.A; SM.A; SA.A; EN.M: Study design, data gathering, data analysis, drafting; All the authors have read and approved the final manuscript and agree to be accountable for all aspects of the work in ensuring that questions related to the accuracy or integrity of any part of the work are appropriately investigated and resolved.

Conflicts of Interest: None declared.

References

1   Beldhuis IE, Lam CSP, Testani JM, Voors AA, Van Spall HGC, Ter Maaten JM, et al. Evidence-Based Medical Therapy in Patients With Heart Failure With Reduced Ejection Fraction and Chronic Kidney Disease. Circulation. 2022;145:693-712. doi: 10.1161/CIRCULATIONAHA.121.052792. PubMed PMID: 35226558; PubMed Central PMCID: PMCPMC9074837.

2   Fujii H, Kono K, Nishi S. Characteristics of coronary artery disease in chronic kidney disease. Clin Exp Nephrol. 2019;23:725-32. doi: 10.1007/s10157-019-01718-5. PubMed PMID: 30830548; PubMed Central PMCID: PMCPMC6511359.

3   Berezina TA, Obradovic Z, Boxhammer E, Berezin AA, Lichtenauer M, Berezin AE. Adropin Predicts Chronic Kidney Disease in Type 2 Diabetes Mellitus Patients with Chronic Heart Failure. J Clin Med. 2023;12. doi: 10.3390/jcm12062231. PubMed PMID: 36983232; PubMed Central PMCID: PMCPMC10059962.

4   Sparks MA, Crowley SD, Gurley SB, Mirotsou M, Coffman TM. Classical Renin-Angiotensin system in kidney physiology. Compr Physiol. 2014;4:1201-28. doi: 10.1002/cphy.c130040. PubMed PMID: 24944035; PubMed Central PMCID: PMCPMC4137912.

5   Casare FA, Thieme K, Costa-Pessoa JM, Rossoni LV, Couto GK, Fernandes FB, et al. Renovascular remodeling and renal injury after extended angiotensin II infusion. Am J Physiol Renal Physiol. 2016;310:F1295-307. doi: 10.1152/ajprenal.00471.2015. PubMed PMID: 26962104.

6   Mikrut K, Kupsz J, Kozlik J, Krauss H, Pruszynska-Oszmalek E, Gibas-Dorna M. Angiotensin-converting enzyme inhibitors reduce oxidative stress intensity in hyperglicemic conditions in rats independently from bradykinin receptor inhibitors. Croat Med J. 2016;57:371-80. doi: 10.3325/cmj.2016.57.371. PubMed PMID: 27586552; PubMed Central PMCID: PMCPMC5048232.

7   Kilkenny C, Browne WJ, Cuthill IC, Emerson M, Altman DG. Improving bioscience research reporting: the ARRIVE guidelines for reporting animal research. Osteoarthritis Cartilage. 2012;20:256-60. doi: 10.1016/j.joca.2012.02.010. PubMed PMID: 22424462.

8   Long DA, Woolf AS, Suda T, Yuan HT. Increased renal angiopoietin-1 expression in folic acid-induced nephrotoxicity in mice. J Am Soc Nephrol. 2001;12:2721-31. doi: 10.1681/ASN.V12122721. PubMed PMID: 11729241.

9   Hrenak J, Arendasova K, Rajkovicova R, Aziriova S, Repova K, Krajcirovicova K, et al. Protective effect of captopril, olmesartan, melatonin and compound 21 on doxorubicin-induced nephrotoxicity in rats. Physiol Res. 2013;62:S181-9. doi: 10.33549/physiolres.932614. PubMed PMID: 24329698.

10 Parasuraman S, Raveendran R. Measurement of invasive blood pressure in rats. J Pharmacol Pharmacother. 2012;3:172-7. doi: 10.4103/0976-500X.95521. PubMed PMID: 22629093; PubMed Central PMCID: PMCPMC3356959.

11 Perrone RD, Madias NE, Levey AS. Serum creatinine as an index of renal function: new insights into old concepts. Clin Chem. 1992;38:1933-53. PubMed PMID: 1394976.

12 Matthews DR, Hosker JP, Rudenski AS, Naylor BA, Treacher DF, Turner RC. Homeostasis model assessment: insulin resistance and beta-cell function from fasting plasma glucose and insulin concentrations in man. Diabetologia. 1985;28:412-9. doi: 10.1007/BF00280883. PubMed PMID: 3899825.

13 Orsolic N, Landeka Jurcevic I, Dikic D, Rogic D, Odeh D, Balta V, et al. Effect of Propolis on Diet-Induced Hyperlipidemia and Atherogenic Indices in Mice. Antioxidants (Basel). 2019;8. doi: 10.3390/antiox8060156. PubMed PMID: 31163593; PubMed Central PMCID: PMCPMC6617317.

14 Cortas NK, Wakid NW. Determination of inorganic nitrate in serum and urine by a kinetic cadmium-reduction method. Clin Chem. 1990;36:1440-3. PubMed PMID: 2387039.

15 Alabiad MA, Harb OA, Hefzi N, Ahmed RZ, Osman G, Shalaby AM, et al. Prognostic and clinicopathological significance of TMEFF2, SMOC-2, and SOX17 expression in endometrial carcinoma. Exp Mol Pathol. 2021;122:104670. doi: 10.1016/j.yexmp.2021.104670. PubMed PMID: 34339705.

16 Ahmed MM, Gebriel MG, Morad EA, Saber IM, Elwan A, Salah M, et al. Expression of Immune Checkpoint Regulators, Cytotoxic T-Lymphocyte Antigen-4, and Programmed Death-Ligand 1 in Epstein-Barr Virus-associated Nasopharyngeal Carcinoma. Appl Immunohistochem Mol Morphol. 2021;29:401-8. doi: 10.1097/PAI.0000000000000903. PubMed PMID: 33480605.

17 Alabiad MA, Harb OA, Taha HF, El Shafaay BS, Gertallah LM, Salama N. Prognostic and Clinic-Pathological Significances of SCF and COX-2 Expression in Inflammatory and Malignant Prostatic Lesions. Pathol Oncol Res. 2019;25:611-24. doi: 10.1007/s12253-018-0534-1. PubMed PMID: 30402808.

18 Alabiad M, Harb O, Mandour D, Hemeda R, R ZA, El-Taher A, et al. Prognostic and clinicopathological implications of expression of Beclin-1 and hypoxia-inducible factor 1alpha in serous ovarian carcinoma: an immunohistochemical study. Pol J Pathol. 2021;72:23-38. doi: 10.5114/pjp.2021.106441. PubMed PMID: 34060285.

19 Suvarna KS, Layton C, Bancroft JD. Bancroft's theory and practice of histological techniques E-Book. Alpharetta: Elsevier health sciences; 2018.

20 Elsalam SA, Mansor AE, Sarhan MH, Shalaby AM, Gobran MA, Alabiad MA. Evaluation of Apoptosis, Proliferation, and Adhesion Molecule Expression in Trophoblastic Tissue of Women With Recurrent Spontaneous Abortion and Infected With Toxoplasma gondii. Int J Gynecol Pathol. 2021;40:124-33. doi: 10.1097/PGP.0000000000000683. PubMed PMID: 32833877.

21 Khayal EE, Alabiad MA, Elkholy MR, Shalaby AM, Nosery Y, El-Sheikh AA. The immune modulatory role of marjoram extract on imidacloprid induced toxic effects in thymus and spleen of adult rats. Toxicology. 2022;471:153174. doi: 10.1016/j.tox.2022.153174. PubMed PMID: 35398170.

22 Shalaby AM, Alnasser SM, Ahmed Khairy D, Alabiad MA, Alorini M, Jaber FA, et al. The neuroprotective effect of ginsenoside Rb1 on the cerebral cortex changes induced by aluminium chloride in a mouse model of Alzheimer's disease: A histological, immunohistochemical, and biochemical study. J Chem Neuroanat. 2023;129:102248. doi: 10.1016/j.jchemneu.2023.102248. PubMed PMID: 36764334.

23 Paradis V, Lagha NB, Zeimoura L, Blanchet P, Eschwege P, Ba N, et al. Expression of vascular endothelial growth factor in renal cell carcinomas. Virchows Arch. 2000;436:351-6. doi: 10.1007/s004280050458. PubMed PMID: 10834538.

24 Akcilar R, Kocak FE, Simsek H, Akcilar A, Bayat Z, Ece E, et al. Antidiabetic and hypolipidemic effects of adropinin streptozotocin-induced type 2 diabetic rats. Bratisl Lek Listy. 2016;117:100-5. doi: 10.4149/bll_2016_020. PubMed PMID: 26830041.

25 Kume T, Calan M, Yilmaz O, Kocabas GU, Yesil P, Temur M, et al. A possible connection between tumor necrosis factor alpha and adropin levels in polycystic ovary syndrome. J Endocrinol Invest. 2016;39:747-54. doi: 10.1007/s40618-016-0453-5. PubMed PMID: 26969461.

26 Kaluzna M, Pawlaczyk K, Schwermer K, Hoppe K, Czlapka-Matyasik M, Ibrahim AY, et al. Adropin and irisin: New biomarkers of cardiac status in patients with end-stage renal disease? A preliminary study. Adv Clin Exp Med. 2019;28:347-53. doi: 10.17219/acem/81538. PubMed PMID: 30525316.

27 Ancion A, Tridetti J, Nguyen Trung ML, Oury C, Lancellotti P. A Review of the Role of Bradykinin and Nitric Oxide in the Cardioprotective Action of Angiotensin-Converting Enzyme Inhibitors: Focus on Perindopril. Cardiol Ther. 2019;8:179-91. doi:

10.1007/s40119-019-00150-w. PubMed PMID: 31578675; PubMed Central PMCID: PMCPMC6828891.

28 Reddy YS, Kiranmayi VS, Bitla AR, Krishna GS, Rao PV, Sivakumar V. Nitric oxide status in patients with chronic kidney disease. Indian J Nephrol. 2015;25:287-91. doi: 10.4103/0971-4065.147376. PubMed PMID: 26628794; PubMed Central PMCID: PMCPMC4588324.

29 Cabarkapa V, Djeric M, Stosic Z, Sakac V, Zagorka LC, Vuckovic B. Evaluation of lipid parameters and bioindices in patients with different stages of chronic renal failure. Vojnosanit Pregl. 2012;69:961-6. PubMed PMID: 23311247.

30 Lamoke F, Mazzone V, Persichini T, Maraschi A, Harris MB, Venema RC, et al. Amyloid beta peptide-induced inhibition of endothelial nitric oxide production involves oxidative stress-mediated constitutive eNOS/HSP90 interaction and disruption of agonist-mediated Akt activation. J Neuroinflammation. 2015;12:84. doi: 10.1186/s12974-015-0304-x. PubMed PMID: 25935150; PubMed Central PMCID: PMCPMC4438457.

31 Gulen B, Eken C, Kucukdagli OT, Serinken M, Kocyigit A, Kilic E, et al. Adropin levels and target organ damage secondary to high blood pressure in the ED. Am J Emerg Med. 2016;34:2061-4. doi: 10.1016/j.ajem.2016.04.014. PubMed PMID: 27592461.

32 Nakashima A, Kato K, Ohkido I, Yokoo T. Role and Treatment of Insulin Resistance in Patients with Chronic Kidney Disease: A Review. Nutrients. 2021;13. doi: 10.3390/nu13124349. PubMed PMID: 34959901; PubMed Central PMCID: PMCPMC8707041.

33 Xu H, Carrero JJ. Insulin resistance in chronic kidney disease. Nephrology (Carlton). 2017;22:31-4. doi: 10.1111/nep.13147. PubMed PMID: 29155496.

34 Valdivielso JM, Rodriguez-Puyol D, Pascual J, Barrios C, Bermudez-Lopez M, Sanchez-Nino MD, et al. Atherosclerosis in Chronic Kidney Disease: More, Less, or Just Different? Arterioscler Thromb Vasc Biol. 2019;39:1938-66. doi: 10.1161/

ATVBAHA.119.312705. PubMed PMID: 31412740.

35 Adejumo OA, Okaka EI, Ojogwu LI. Lipid profile in pre-dialysis chronic kidney disease patients in southern Nigeria. Ghana Med J. 2016;50:44-9. doi: 10.4314/gmj.v50i1.7. PubMed PMID: 27605724; PubMed Central PMCID: PMCPMC4994483.

36 Amdur RL, Feldman HI, Dominic EA, Anderson AH, Beddhu S, Rahman M, et al. Use of Measures of Inflammation and Kidney Function for Prediction of Atherosclerotic Vascular Disease Events and Death in Patients With CKD: Findings From the CRIC Study. Am J Kidney Dis. 2019;73:344-53. doi: 10.1053/j.ajkd.2018.09.012. PubMed PMID: 30545708; PubMed Central PMCID: PMCPMC6812505.

37 Bo MS, Cheah WL, Lwin S, Moe Nwe T, Win TT, Aung M. Understanding the Relationship between Atherogenic Index of Plasma and Cardiovascular Disease Risk Factors among Staff of an University in Malaysia. J Nutr Metab. 2018;2018:7027624. doi: 10.1155/2018/7027624. PubMed PMID: 30116641; PubMed Central PMCID: PMCPMC6079547.

38 Apple FS, Collinson PO, Biomarkers ITFoCAoC. Analytical characteristics of high-sensitivity cardiac troponin assays. Clin Chem. 2012;58:54-61. doi: 10.1373/clinchem.2011.165795. PubMed PMID: 21965555.

39 Simes J, Robledo KP, White HD, Espinoza D, Stewart RA, Sullivan DR, et al. D-Dimer Predicts Long-Term Cause-Specific Mortality, Cardiovascular Events, and Cancer in Patients With Stable Coronary Heart Disease: LIPID Study. Circulation. 2018;138:712-23. doi: 10.1161/CIRCULATIONAHA.117.029901. PubMed PMID: 29367425.

40 Carlstrom M. Nitric oxide signalling in kidney regulation and cardiometabolic health. Nat Rev Nephrol. 2021;17:575-90. doi: 10.1038/s41581-021-00429-z. PubMed PMID: 34075241; PubMed Central PMCID: PMCPMC8169406.